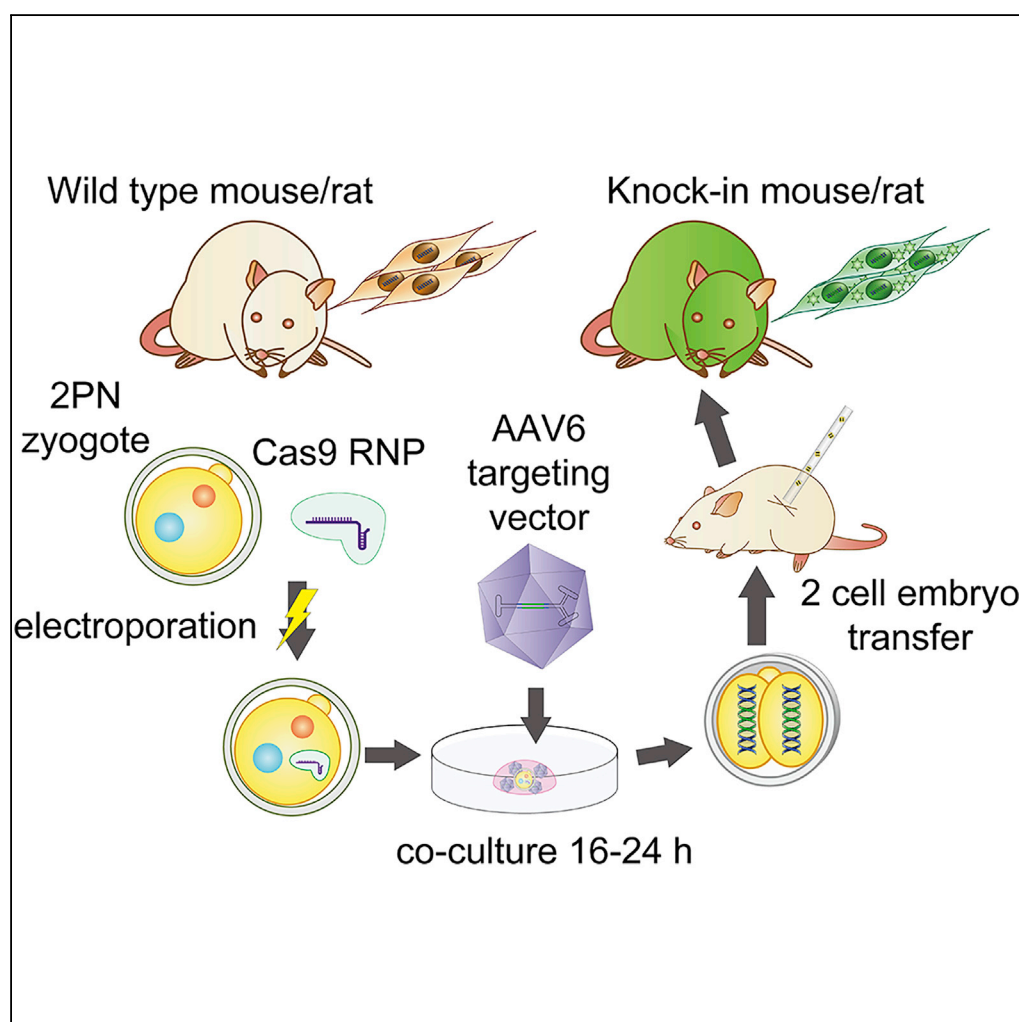**Article**

Intra-embryo Gene Cassette Knockin by CRISPR/Cas9-Mediated Genome Editing with Adeno-Associated Viral Vector

Naoaki Mizuno, Eiji Mizutani, Hideyuki Sato, ..., Fabian Suchy, Tomoyuki Yamaguchi, Hiromitsu Nakauchi

tomoyama@ims.u-tokyo.ac.jp (T.Y.)
nakauchi@stanford.edu (H.N.)

HIGHLIGHTS

AAV infects zygotes of various mammals through intact zona pellucida

AAV vector delivers large knockin cassettes into zygotes without micromanipulation

Cas9 RNP electroporation and donor AAV enable efficient intra-embryo knockin

Article

Intra-embryo Gene Cassette Knockin by CRISPR/Cas9-Mediated Genome Editing with Adeno-Associated Viral Vector

Naoaki Mizuno,[1] Eiji Mizutani,[1] Hideyuki Sato,[1] Mariko Kasai,[1] Aki Ogawa,[1] Fabian Suchy,[2] Tomoyuki Yamaguchi,[1,3,*] and Hiromitsu Nakauchi[1,2,*]

SUMMARY

Intra-embryo genome editing by CRISPR/Cas9 enables easy generation of gene-modified animals by non-homologous end joining (NHEJ)-mediated frameshift mutations or homology-directed repair (HDR)-mediated point mutations. However, large modifications, such as gene replacement or gene fusions, are still difficult to introduce in embryos without costly micromanipulators. Moreover, micromanipulation techniques for intra-embryo genome editing have been established in only a small set of animals. To overcome these issues, we developed a method of large-fragment DNA knockin without micromanipulation. In this study, we successfully delivered the knockin donor DNA into zygotes by adeno-associated virus (AAV) without removing the zona pellucida, and we succeeded in both large-DNA fragment knockin and whole exon exchange with electroporation of CRISPR/Cas9 ribonucleoprotein. By this method, we can exchange large DNA fragments conveniently in various animal species without micromanipulation.

INTRODUCTION

Genome editing techniques, especially clustered regularly interspaced short palindromic repeats/CRISPR-associated protein 9 (CRISPR/Cas9) technology, have significantly simplified the creation of genetically modified cells and animals. CRISPR/Cas9 utilizes programmable nucleases that form a complex with a guide RNA (gRNA). The ribonucleoprotein (RNP) utilizes the RNA to target a specific site in any chromosome and produce a double-stranded break (DSB). The DSB is repaired by non-homologous end joining (NHEJ), homology-directed repair (HDR), or microhomology-mediated end joining (MMEJ). In the NHEJ pathway mediated by Ku70/Ku80, the ends of the DSB are combined with small insertions or deletions. In MMEJ, microhomology near the cleavage site is annealed and repaired with a small defect. Both NHEJ and MMEJ repair mechanisms are imperfect and may cause a frameshift mutation, thereby destroying the function of the gene. In contrast, targeted gene knockins are used to integrate reporter genes downstream of desired promoters, insert gene expression cassettes into safe harbors such as the Rosa26 or AAVS1 loci, or exchange large regions of DNA such as an exon. Although knockins are mainly carried out by HDR-mediated repair mechanisms, MMEJ-mediated target gene integration method (precise integration into target chromosome) and NHEJ-mediated target gene integration (homology-independent targeted integration) have been recently developed (Sakuma et al., 2015; Suzuki et al., 2016). All methods of knockin require delivery of donor DNA into the cell nucleus in addition to the CRISPR/Cas9 complex.

Genetically modified rodents are often developed by first producing embryonic stem (ES) cells with the desired genotype. These cells are selected and injected into embryos, producing chimeric pups. If the injected cells contributed to the germline, the rodents can be mated to produce new offspring with the intended genotype. This process requires multiple generations of animals and can be inefficient. Genome editing performed in zygotes could produce genetically modified animals in the first generation. This would enable site-directed transgenesis even in non-rodent mammals, from which ES cells have not been shown to contribute to germline chimeras.

Genetically modifying zygotes can be achieved by somatic cell nuclear transfer or direct injection of CRISPR/Cas9. This requires advanced training and expensive micromanipulation equipment. Alternatively, RNP-mediated editing in zygotes can be performed by electroporation of the CRISPR/Cas9 complex

(Kaneko and Mashimo, 2015); however, large templates of donor DNA cannot be transfected as efficiently (Chen et al., 2016; Hashimoto et al., 2016). Thus, simple gene modifications in zygotes are limited in adaptation to point mutation/repair or small insertions/deletions and require specific gRNAs for each mutated sequence. These small modifications are not sufficient for all applications including disease modeling, as it is difficult to faithfully reproduce disease phenotypes caused by large insertions/deletions. To overcome this issue, technology for replacing a large fragment, such as a whole exon, is necessary. Although genome editing technology has made it easy to generate genetically modified cells, it is still difficult to add or replace large fragments in fertilized embryos.

RESULTS

Trans-Zona Pellucida DNA Delivery by AAV Vector

To stably deliver the donor DNA for gene knockin into the nucleus, a viral vector whose genome is covered with a capsid is suitable. Because adeno-associated viral (AAV) vectors, adenoviral vectors, and lentiviral vectors are commonly used as gene delivery vehicles for experimental and therapeutic applications, the infectivity of these viral vectors on embryos was first confirmed. For AAV, we chose the serotype 6 AAV (AAV6) vector based on its infectivity in mouse and human ES cells as previously reported (Ellis et al., 2013).

In earlier studies, embryos were infected with viral particles by microinjecting the virus into the perivitelline space. Therefore, each viral vector (AAV, adenoviral, and lentiviral) encoding enhanced green fluorescent protein (EGFP) driven by the CAG promoter was microinjected into the perivitelline space of pronuclear-stage mouse embryos, and the expression of EGFP was confirmed under a fluorescence microscope at the morula/blastocyst stage. The infection was confirmed with adenoviral and lentiviral vectors; however, transgene expression was not obvious in embryos with AAV vector (Figures 1I, 1J, S1C–S1F, S2C, and S2D). Removal of the zona pellucida also enabled efficient infection by the lentiviral vector as reported previously (Figures S1G and S1H) (Ikawa et al., 2003).

As a control, embryos with an intact zona pellucida were co-cultured with the viral vectors, resulting in no infection with lentiviral or adenoviral vectors as expected (Figures S1A, S1B, S2A, and S2B). However, efficient infection was observed with the AAV vector (Figures 1A and 1B). Transgene expression was AAV vector dose-dependent, and high from the 4-cell stage to the morula stage in mice embryos (Figure S3). We also confirmed AAV serotypes other than serotype 6, and AAV6 showed the highest transduction efficiency (Figure S4). Moreover, we examined rat embryos and bovine embryos for AAV transduction. AAV6 transduced both of them efficiently. Since the zona pellucida was thought to be a defense against viral infection, we assumed that this infection was established by the virus passing through the holes created during fertilization. To test this hypothesis, we infected parthenogenetic embryos with the AAV vector, and unexpectedly the infection was established (Figures 1E–1H). These results indicate that the AAV vector can pass through the intact zona pellucida and infect the embryos. This is consistent with the result of AAV microinjection into perivitelline space. We could inject femto-picoliter virus suspension at 1×10^8 IU/mL, which is equivalent to 1×10^{10} vg/mL = 10 vg/pL, into the perivitelline space of each zygote. If zona pellucida is a barrier for virion transmission, all virions might be enclosed in the perivitelline space until zygote infection, and such small amount of virion would be enough for zygote transduction, as in case of other viral vectors. In case of AAV, virion would be diffused from perivitelline space into the culture media, and the multiplicity of infection (MOI) would be insufficient for zygote transduction.

The zona pellucida of mammals is divided into three types depending on the type of constituent glycoprotein. The zona pellucida of mice consists of ZP1, ZP2, and ZP3; the zona pellucidae of humans and rats consist of ZP1, ZP2, ZP3, and ZP4; and the zona pellucida of cattle consists of ZP2, ZP3, and ZP4 (Izquierdo-Rico et al., 2009). We found that the AAV vector can pass through both rat and bovine zona pellucidae to efficiently infect the embryo (Figures 1K–1R). The results indicate that the AAV vector is suitable for delivering donor DNA to the fertilized eggs of any mammalian species without the need for micromanipulation.

Mouse *Rosa26* Locus Knockin with AAV Vector

We investigated whether the delivery of donor DNA into embryos by the AAV vector is effective for large-fragment knockin using the CRISPR/Cas9 system. After introducing the Cas9-RNP into pronuclear-stage embryos by electroporation, we infected with a self-complementary AAV (scAAV) vector harboring a 1.8-kb CAG-GFP cassette flanked by two 100-bp *Rosa26* homology arms (2 kb in total) (Figures 2A
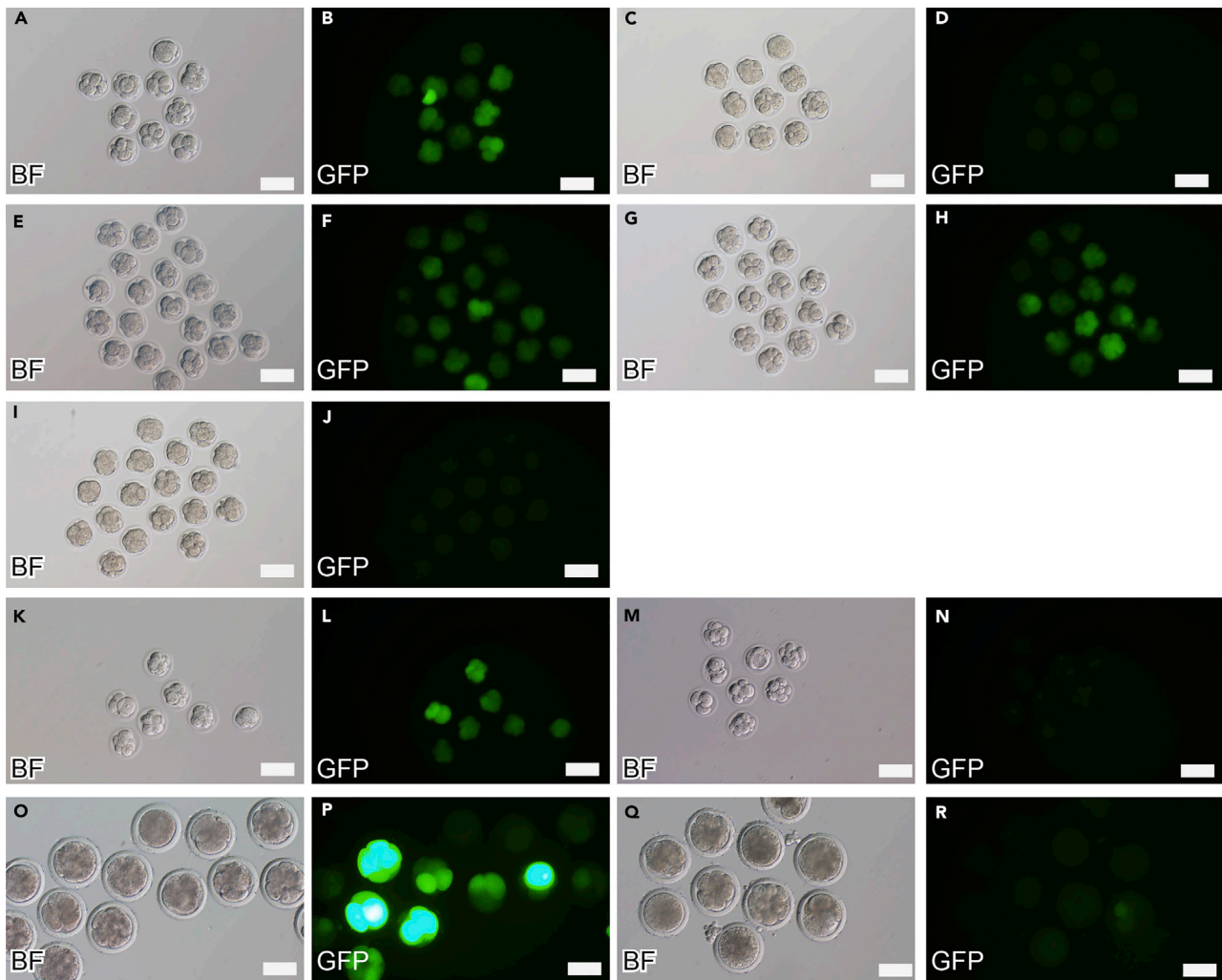
Figure 1. AAV-Mediated Transduction of Embryos with Zona Pellucida

(A–J) Zygotes of mice were co-cultured with EGFP-expressing scAAV6 for 16–24 hr. The expression of EGFP was analyzed by fluorescence microscopy from morula to blastocyst stage. The fertilized zygotes co-cultured with scAAV6-CAG-EGFP at a concentration of 1×10^5 IU/mL (A and B) showed high EGFP expression compared with that of the mock-treated embryos (C and D). Parthenogenetic oocytes exposed to scAAV6-CAG-EGFP after activation at 1×10^5 IU/mL for 16 hr (E and F) and before activation at 1×10^6 IU/mL for 1 hr (G and H) also showed EGFP expression. Microinjection of AAV at a concentration of 1×10^8 IU/mL to perivitelline space shows no EGFP expression (I and J).

(K–R) Fertilized zygotes of rats (K and L) and cattle (O and P) co-cultured with scAAV6-CAG-EGFP at a concentration of 1×10^6 IU/mL for 16–24 hr also resulted in high EGFP expression compared with that of mock-transduced embryos of rats (M and N) and cattle (Q and R).

Scale bars, 100 μm. See also Figures S1–S4.

and 2B). At the blastocyst stage, the efficiency of knockin in the *Rosa26* locus was 15.5%, and the concentration of scAAV did not affect the efficiency of knockin (Table 1). The birth rate of offspring was 19.3%, of which 6.3% had the cassette inserted into the *Rosa26* locus (Table 2). EGFP expression was confirmed by fluorescence stereomicroscopy and flow cytometry of peripheral blood (Figures 2C, 2D, and 2F). Moreover, we found that the cassette was correctly inserted in the *Rosa26* locus without indel mutations at the site of junction (Figures 2E and S5A). Germline transmission was confirmed by breeding the knockin founders and wild-type C57BL/6N mice, followed by genotyping of N1 generation offsprings (Figure S7A).

Furthermore, we performed the same experiment with single-strand AAV (ssAAV) vector harboring a 1.8-kb CAG-GFP cassette flanked by two 1-kb *Rosa26* homology arms (3.8 kb in total) (Figure 2G). The birth rate of offspring was 34.5%, and the rate of *Rosa26* locus insertion in offspring was 13.8% (Table 2). EGFP expression was confirmed by fluorescence stereomicroscopy and flow cytometry of peripheral blood (Figure 2I). The
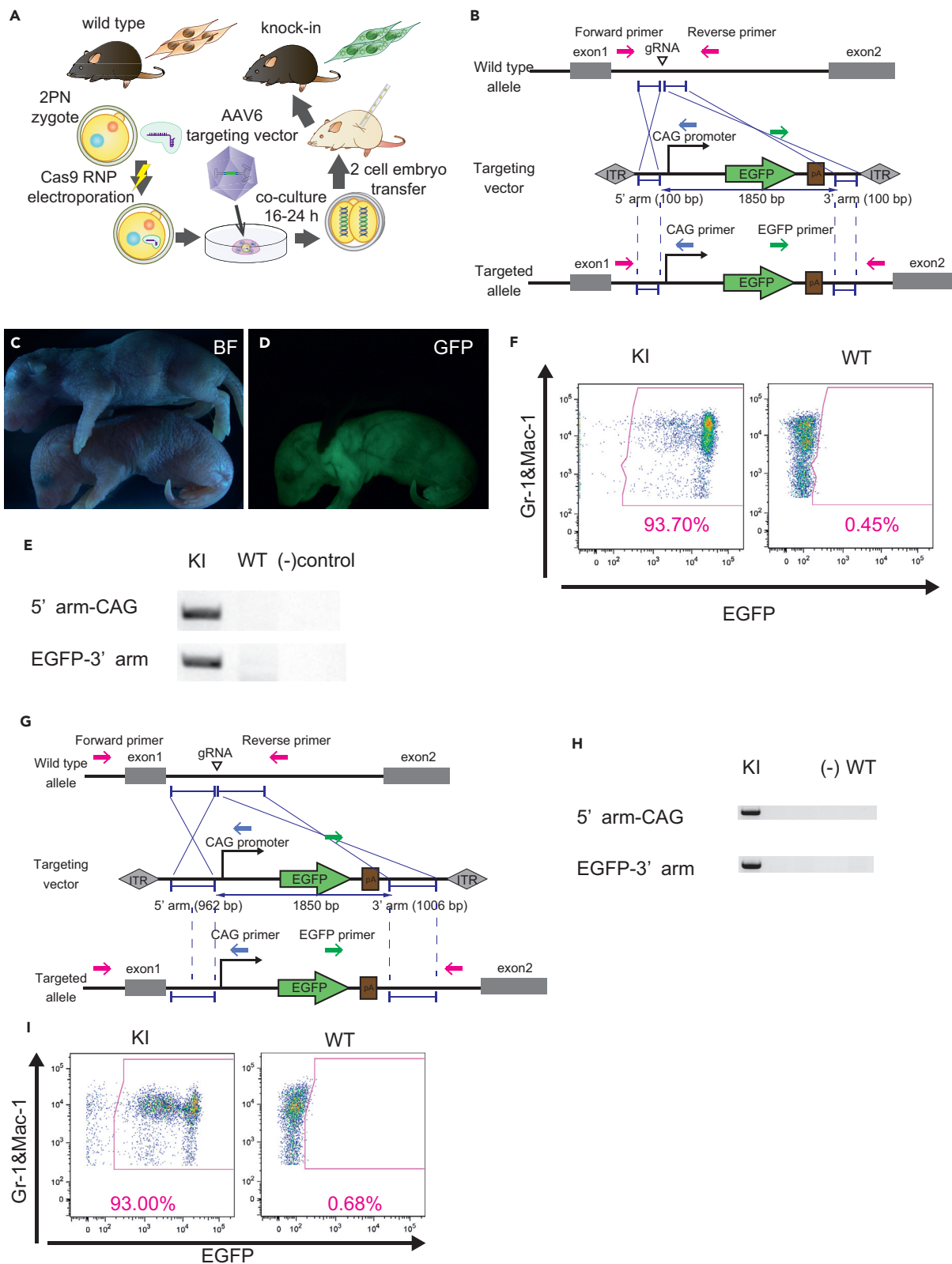
Figure 2. Large-Fragment Knockin by Donor AAV Transduction and CRISPR/Cas9 RNP Electroporation in Mouse Embryos

(A–F) Knockin by scAAV donor vector. (A) Schematic representation of knockin for *Rosa26* locus. Two pronuclear embryos of wild-type mice were electroporated with Cas9 protein and gRNA targeting the *Rosa26* locus and cultured *in vitro* for 16–24 hr with donor AAV6. The embryos that developed normally to the 2-cell stage were collected and transferred to oviducts of surrogate mothers. (B) Donor scAAV vector containing 1,850-bp CAG-EGFP cassette flanked by approximately 100-bp homology arms next to the gRNA target. Magenta arrows, mouse *Rosa26* primers (forward and reverse); blue arrow, CAG promoter primer; green arrow, EGFP primer. (C and D) Fluorescence stereomicroscopy of knockin and wild-type neonates. (E) Representative of genotyping of knockin mice. Primers flank the 5′- and 3′-junctional regions. (F) Flow cytometry of peripheral blood myeloid cells.

(G–I) Knockin by ssAAV donor vector. (G) Donor ssAAV vector containing 1,850-bp CAG-EGFP cassette flanked by approximately 1,000-bp homology arms next to the gRNA target. Magenta arrows, mouse *Rosa26* primers (forward and reverse); blue arrow, CAG promoter primer; green arrow, EGFP primer. (H) Representative of genotyping of knockin mice by ssAAV. Primers flank the 5′- and 3′-junctional regions. (I) Flow cytometry of peripheral blood myeloid cells.

See also Figures S5, S7A, and S7B.

cassette was correctly inserted in the *Rosa26* locus without indel mutations at the site of junction (Figures 2H and S5B). Germline transmission was confirmed by breeding the knockin founders and wild-type C57BL/6N mice, followed by genotyping of N1 generation offsprings (Figure S7B). Some offspring showed positive genotype either at the 5′ or 3′ junction of the mouse *Rosa26* knockin allele (Table 2). We could not identify the whole sequences at those integration sites. This might be partly due to non-HDR integration of AAV donor with ITR (Inverted Terminal Repeat), whose secondary structure hampers PCR. However, we could not determine vector-derived sequences, even by PCR with 7-deaza-dGTP, which improves PCR for AAV-ITR (data not shown) (Mroske et al., 2012). We could not rule out intra-vector deletion of concatemeric insertion either (Nowrouzi et al., 2012).

These results indicate that both scAAV and ssAAV vectors can stably deliver a large fragment of donor DNA for CRISPR/Cas9-mediated site-specific knockin without micromanipulation.

Rat *Rosa26* Locus Knockin with AAV Vector

We next examined the knockin efficiency in rat embryos. Similar to the experiment described above, the scAAV vector harboring 1.8-kb CAG-GFP cassette flanked by two 100-bp *Rosa26* homology arms (2 kb in total) was injected into the rat embryo after electroporation with Cas9-RNP (Figure 3A). The birth rate of offspring was 16.7%, and the rate of *Rosa26* locus insertion in offspring was 25.0% (Table 3). We also found that the cassette was correctly inserted in the *Rosa26* locus without indel mutations at the site of junction as described above (Figures 3B and S6). The EGFP expression of the rat in which the knockin cassette was correctly inserted was confirmed by fluorescence stereomicroscopy and flow cytometry of peripheral blood (Figures 3C–3E). Germline transmission was confirmed by breeding the knockin founders and wild-type Wistar rats, followed by genotyping of N1 generation offsprings (Figure S7C).

We also performed the same experiment with ssAAV vector harboring a 1.8-kb CAG-GFP cassette flanked by two 1-kb *Rosa26* homology arms (3.8 kb in total) (Figure 3F). The birth rate of offspring was 5.4%, and the rate of *Rosa26* locus insertion in offspring was 100% (Figure 3G and Table 3). EGFP expression was confirmed by fluorescence stereomicroscopy and flow cytometry of peripheral blood (Figure 3I). The cassette was correctly inserted in the *Rosa26* locus without indel mutations at the site of junction (data not shown).

Moreover, droplet digital PCR was used to quantify the number of EGFP inserts and wild-type (un-inserted) *Rosa26* alleles per cell (Figure 3H). Three of the five knockin offsprings (#1, #2, and #5) in scAAV group showed inconsistent copy numbers of transgene and uninserted *Rosa26* allele. The copy numbers per cell were not integer in those cases. This indicates that they were definitely mosaic, despite none of the three in ssAAV. After germline transmission, offsprings of the knockin founder with 1.3 EGFP copies/cell (#1 in Figure 3H) had integer copies per cell of EGFP from 0 to 2 (Figure S7D). Flow cytometry of white blood cells in peripheral blood showed consistent phenotypes of the mosaic offsprings on droplet digital PCR (Figure 3I).

These results indicate that the trans-zona pellucida donor DNA delivery by AAV vector is effective for large-fragment knockin in the *Rosa26* locus even in the rat embryo whose zona pellucida consists of different components than mouse. However, mosaicism of off-target integration was also observed.

Rescue of the Nude Phenotype by Exon Exchange

The nude (*Foxn1^nu*) mutation, which is a single base pair (G) deletion in exon 3, results in a frameshift mutation that induces an athymic and hairless phenotype. To rescue the nude phenotype by exon exchange

Vector Type	AAV Concentration	Number of 2PN Zygotes Treated	Number of Zygotes in Blastocyst Stage	Number of Zygotes Genotyped	Number of Knockin Embryos[a]	Number of Embryos with Partial Insertion[b]
scAAV6	1×10^5 IU/mL	80	53 (66.3)	47 (88.7)	7 (14.9)	4 (8.5)
scAAV6	1×10^6 IU/mL	40	29 (72.5)	24 (82.8)	4 (16.7)	1 (4.2)
ssAAV6	1×10^7 vg/mL	21	18 (85.7)	18 (100)	2 (11.1)	2 (11.1)
ssAAV6	1×10^8 vg/mL	12	7 (58.3)	7 (100)	0 (0)	3 (42.9)

Table 1. Knockin Efficiency of *In Vitro*-Cultured Mouse Blastocyst after Zygote Genome Editing with Donor AAV Transduction

[a]Embryos with positive genotype at both 5′ and 3′ junctions of the mouse *Rosa26* knockin allele.
[b]Embryos with positive genotype at either 5′ or 3′ junction of the mouse *Rosa26* knockin allele.

using a large-fragment knockin technique, we designed gRNAs to target 420 bp upstream (intron 2) and 550 bp downstream (intron 3) of the mutation in exon 3 and generated scAAV harboring functional exon 3 (462 bp) flanked by two homology arms (434 and 400 bp) (Figure 4A). After introducing the Cas9-RNP into pronuclear-stage embryos by electroporation, we infected with the scAAV vector harboring the donor DNA cassette. The birth rate was 20.3%, with exon exchange in 13.8% of the offspring (Table S1). Successful exchange of exon 3 was confirmed by Sanger sequencing and restriction fragment-length polymorphism analysis (Figures 4C and 4D). Furthermore, the restoration of hairless phenotype was observed in all mice with exchanged wild-type exon 3 (Figure 4B). Flow cytometry revealed that the CD3+ T lymphocytes were recovered in the peripheral blood of a mouse with exchanged exon 3: 16.04% ± 3.97%, 0.44% ± 0.22%, 0.72% ± 0.11% in KSN/Slc-*Foxn1*^*repaired/nu*^, KSN/Slc-*Foxn1*^*Δexon3/nu*^, KSN/Slc-*Foxn1*^*nu/nu*^ (mean ± SEM, n = 3, 8, 4), respectively. The CD3+ T cells in KSN/Slc-*Foxn1*^*repaired/nu*^ showed CD4+CD8 or CD8+CD4 phenotypes as mature T cells in wild-type mice (Figure 4E). These results indicate that an intact exon can be exchanged by CRISPR/Cas9-mediated large-fragment knockin in embryos. In addition, the repaired *Foxn1* allele was conserved in the next generation (Figure S7E).

DISCUSSION

In the present study, we successfully performed large-fragment genome editing in embryos via CRISPR/Cas9 and trans-zona pellucida delivery of donor DNA with AAV vectors.

There is a little evidence regarding viral infection in preimplantation embryos with an intact zona pellucida. Bane et al. reported that porcine parvovirus can infect preimplantation porcine embryos with intra-embryonic replication of the viral genome (Bane et al., 1990). While we conducted our study, other groups also demonstrated that the AAV vector can pass through the zona pellucida (Yoon et al., 2018). Previous structural analysis of bovine zona pellucida showed that the average pore size of bovine zona pellucida is about 223 nm, and that 40-nm beads can enter halfway through the zona pellucida (Vanroose et al., 2000). The porcine parvovirus and AAV are relatively small viruses of about 20 nm belonging to the family Parvoviridae. Furthermore, a previous study showed that 20- to –40-nm-sized multi-walled carbon nanotubes can deliver DNA through the zona pellucida (Munk et al., 2016). Therefore, the size of the virus might be a key factor for translocation through zona pellucida, and other viruses with size <20 nm will likely pass through the zona pellucida.

We observed fluorescent reporter gene expression in mouse embryos infected by serotype 6 or serotype 1 AAV, whereas expression was not detected in serotype 2 AAV-infected embryos (Figures S4A, S4D, S4G,

Vector Type	AAV Concentration	Number of 2PN Zygotes Treated	Number of Zygotes in 2-Cell Stage	Number of Zygotes Transferred	Number of Offsprings	Number of Knockin Offsprings[a]	Number of Offsprings with Partial Insertion[b]
scAAV6	1×10^5 IU/mL	370	265 (71.6)	166 (62.6)	32 (19.3)	2 (6.3)	8 (25)
ssAAV6	1×10^7 vg/ml	109	93 (85.3)	84 (90.3)	29 (34.5)	4 (13.8)	1 (3.4)

Table 2. Knockin Efficiency of Mouse Offspring after Zygote Genome Editing with Donor AAV Transduction

[a]Offspring with positive genotype at both 5′ and 3′ junctions of the mouse *Rosa26* knockin allele.
[b]Offspring with positive genotype at either 5′ or 3′ junction of the mouse *Rosa26* knockin allele.
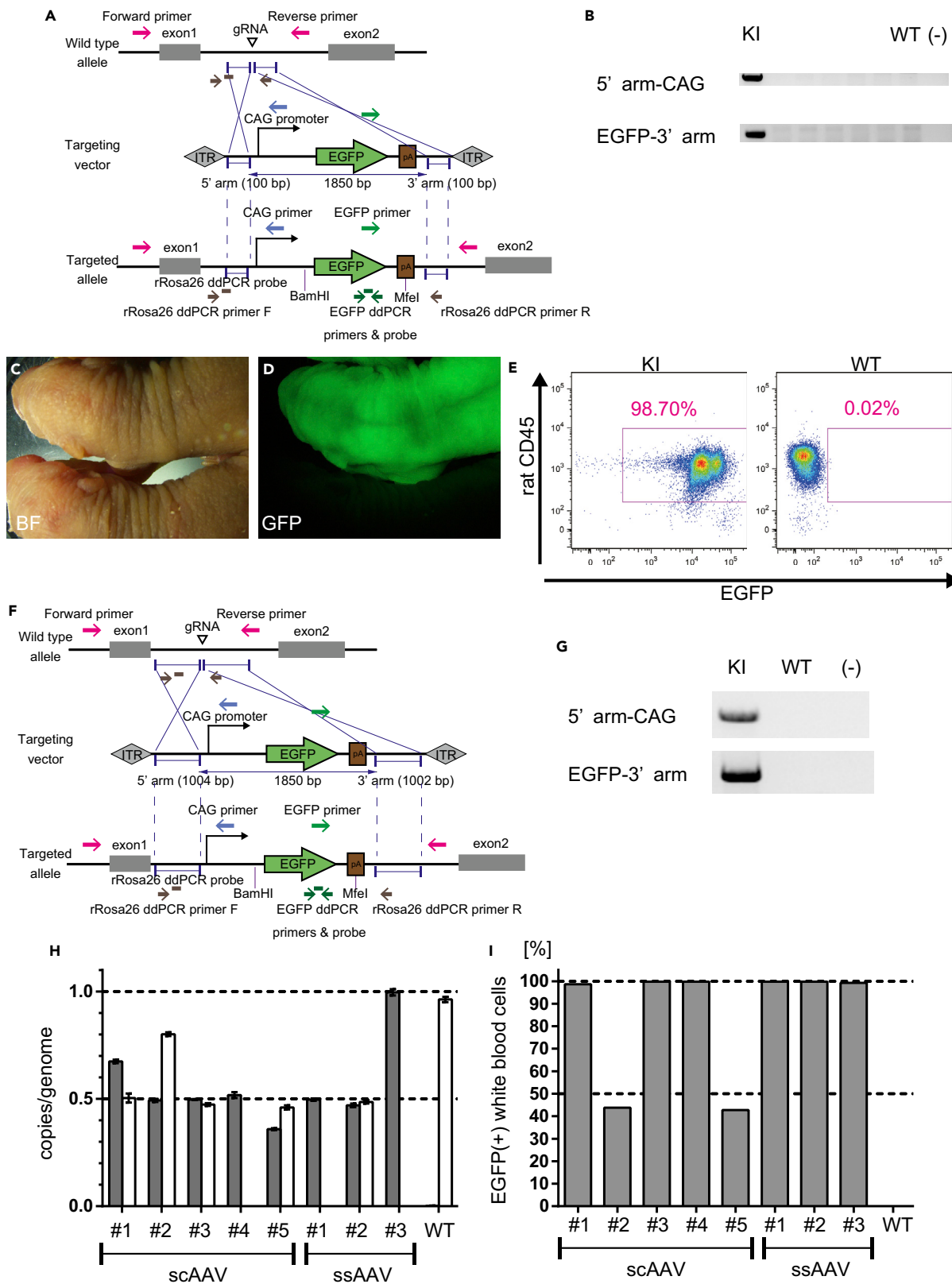
Figure 3. Large-Fragment Knockin by Donor AAV Transduction and CRISPR/Cas9 RNP Electroporation in Rat Embryos

(A–E) Knockin by scAAV donor vector. (A) Schematic representation of targeting strategy. Donor scAAV vector containing 1,850-bp CAG-EGFP cassette flanked by approximately 100-bp homology arms next to the gRNA target. Magenta arrows, rat *Rosa26* primers (forward and reverse); blue arrow, CAG promoter primer; green arrow, EGFP primer; brown arrow, rat *Rosa26* primers (forward and reverse) for droplet digital PCR; brown line, rat *Rosa26* probe for droplet digital PCR; dark green allow, EGFP primers (forward and reverse) for droplet digital PCR; dark green line, EGFP probe for droplet digital PCR. (B) Representative of genotyping of knockin rat. Primers flanked the 5′- and 3′-junctional regions. (C and D) Fluorescence stereomicroscopy of knockin and wild-type neonates. (E) Flow cytometry of peripheral blood white blood cells. CD45-positive cells in knockin rat show EGFP expression.

(F–G) Knockin by ssAAV donor vector. (F) Donor ssAAV vector containing 1,850-bp CAG-EGFP cassette flanked by approximately 1,000-bp homology arms next to the gRNA target. Magenta arrows, rat *Rosa26* primers (forward and reverse); blue arrow, CAG promoter primer; green arrow, EGFP primer; brown arrow, rat *Rosa26* primers (forward and reverse) for droplet digital PCR; brown line, rat *Rosa26* probe for droplet digital PCR; dark green arrow, EGFP primers (forward and reverse) for droplet digital PCR; dark green line, EGFP probe for droplet digital PCR. (G) Representative of genotyping of knockin rat by ssAAV. Primers flank the 5′- and 3′-junctional regions. (H) Copy number quantification of EGFP and rat *Rosa26* allele without integration by droplet digital PCR. Absolute copies were normalized to copies of reference genome targeting endogenous *Zeb2* locus and expressed as mean $\pm$ SEM (n = 4, technical replicates). Gray column, EGFP copies/genome; open column, copies of uninserted rat *Rosa26* allele/genome. (I) Frequency of EGFP-positive cells in peripheral blood CD45+ cells of the knockin rats, assessed by flow cytometry.

See also Figures S6, S7C, and S7D.

and S4J). Yoon et al. performed similar infection experiments in morula-stage mouse embryos and observed efficient gene expression in serotype 2 AAV-infected embryos (Yoon et al., 2018). This might be due to the difference in infection timing, MOI, or fluorescence detection sensitivity. We also detected higher reporter gene expression in rat embryos infected by AAV6 than those infected by AAV1 or AAV2 (Figures S4B, S4E, S4H, and S4K). Interestingly, bovine embryos were transduced with AAV2 as well as AAV1 and AAV6 (Figures S4C, S4F, S4I, and S4L). Our data indicate that serotype 6 AAV might be promising for zygote transduction in a variety of mammals; however, AAV-serotype-specific tropism for zygotes differs among species. Off-target integration and mosaicism were inferred from droplet digital PCR-based trans-gene copy number analysis. Since the AAV genome can be episomally maintained for a long time, it might be possible for additional insertions to occur after the one-cell stage of embryo development, leading to mosaicism.

Since AAV is nonpathogenic, efficiently infects non-dividing cells, and yields prolonged gene expression, the AAV vector has gained attention in the field of gene therapy. However, there is a concern that AAV might infect germ cells *in vivo* as it passes through the zona pellucida. At least one previous study has reported that the AAV genome was detected in male germ cells (Erles et al., 2001). Moreover, although *Rep* is deleted in the AAV vector, integration of the AAV genome into host's chromosomes has been reported (Gil-Farina et al., 2016; Kaeppel et al., 2013). Our data indicate that the AAV vector will likely pass through human zona pellucida and thus warrants consideration while using AAV vectors for gene therapy to avoid genome integration in germ cells.

When generating multiple mutations in one exon for purposes such as disease modeling, we propose that it may be easier to replace an entire exon instead of targeting each mutation individually. This strategy can also be used to repair structural variants, including fusion genes following translocation events or large insertions/deletions, other than just point mutations. Even for gene correction of point mutations, large fragment exchange strategy might be beneficial in some cases. Although point mutation correction by genome editing with single-strand oligodeoxynucleotide would be the best way in many cases, we have to design fine gRNA close to mutations. We can design gRNAs more flexibly around mutation hotspots with large-fragment knockin method, and we would employ the same gRNAs for patients with different point mutation on the same hotspot. The utility of embryonic gene therapy is not limited to humans. Because of inbreeding, genetic diseases are increasing in livestock animals, increasing the demand for livestock gene therapy.

Although several previous studies have succeeded in large-fragment knockin in mouse embryos with similar efficiency (5%–45%) as our AAV-mediated method (6.3%–100%), they delivered CRISPR/Cas9 and donor DNA by pronuclear microinjection (Aida et al., 2015; Miura et al., 2017; Yang et al., 2013; Yoshimi et al., 2016). Recently, Miyasaka et al. succeeded in introducing large fragment into rodent zygotes by electroporation of long single-strand donor DNA without micromanipulation; however, the donor DNA were up to 1.1 kb, including homology arms (Miyasaka et al., 2018). Pronuclear injection is a highly skilled technique and relatively difficult in non-rodent mammals. For example, in bovine or porcine embryos, it is difficult to identify the pronucleus by conventional methods because it is masked by lipid droplets. Our

Vector Type	AAV Concentration	Number of 2PN Zygotes Treated	Number of Zygotes in 2-Cell Stage	Number of Zygotes Transferred	Number of Offsprings	Number of Knockin Offsprings[a]	Number of Offsprings with Partial Insertion[b]
scAAV6	1×10^5 IU/mL	139	120 (86.3)	120 (100)	20 (16.7)	5 (25)	0 (0)
ssAAV6	1×10^7 vg/ml	60	56 (93.3)	56 (100)	3 (5.4)	3 (100)	0 (0)

Table 3. Knockin Efficiency of Rat Offspring after Zygote Genome Editing with Donor AAV Transduction
[a]Offspring with positive genotype at both 5′ and 3′ junctions of the rat *Rosa26* knockin allele.
[b]Offspring with positive genotype at either 5′ or 3′ junction of the rat *Rosa26* knockin allele.

strategy does not require advanced techniques or special equipment such as micromanipulators, and many embryos can be processed simultaneously. Moreover, we could apply the same strategy to non-rodent mammals, in which germline-competent pluripotent stem cells have not been reported, enabling us to establish disease models with mammals that are more similar to those with humans genetically and physiologically. The genome of wild-type AAV is about 4.7 kb, and recombinant AAV vector has a packaging capacity of around 5.2 kb (Grieger and Samulski, 2005; Wu et al., 2010). Since we succeeded in introducing large exogenous fragment by scAAV with 100-bp homology arms and ssAAV with 1-kb homology arms, the donor AAV could contain up to 4.7-kb-length exogenous fragment theoretically. However, ssAAV with longer homology arms showed higher efficiency for precise knockin (Tables 2 and 3). The length of homology arms could affect it, and exogenous cassette would be shortened practically. Micromanipulation is still necessary for the introduction of >5.2-kb fragment. However, inter-AAV genomic homologous recombination could potentially serve longer donor DNA (Bak and Porteus, 2017; Wu et al., 2010).

It seems a good alternative to introduce Cas9 and gRNA by AAV vector. However, we could not expect Cas9 expression in 1-cell stage. Following mice zygote transduction with CAG-EGFP-expressing scAAV6, we could detect very low EGFP fluorescence under microscopy in the 2-cell stage, whereas embryos showed extremely high EGFP fluorescence after the 4-cell stage (Figure S3). Transgene expression from exogenous DNA depends on the embryo's transcription/translation machinery. In mouse zygotes, transcription from zygote genome is repressed in early 1-cell stage, and activated from late 1- to 2-cell stage (Abe et al., 2018; Jukam et al., 2017; Wiekowski et al., 1991). Minor zygotic activation occurred at the late 1-cell stage, whereas major zygotic activation and translation start from the 2-cell stage. These findings on zygotic genome activation explain the time course of EGFP reporter expression. In addition, Cas9 coding sequence is too large for scAAV, which has a capacity limitation of 2.3–2.5 kb. Even for smaller Cas9, including SaCas9, we have to use conventional ssAAV vector. Because transgene expression from ssAAV is much slower than scAAV, Cas9 expression from ssAAV would be insufficient in the 1-cell stage (McCarty et al., 2001; Wang et al., 2003). More importantly, zygotic genome activation starts at a later stage in other mammalian species (e.g., 4-to 8-cell stage in humans). Genome editing by Cas9 RNP electroporation has reduced the risk of mosaicism in rodent zygotes (Chen et al., 2016; Hashimoto et al., 2016; Kaneko and Mashimo, 2015). Cas9 and gRNA introduction by AAV vector might be simpler than Cas9 RNP electroporation, but might cause more mosaic, especially in other animals. The combination of donor DNA introduction by AAV vector and CRISPR/Cas9 genome editing by RNP electroporation could be applied to a multitude of species for both research and therapeutic purposes.

Limitations of the Study

Optimal conditions for embryos co-culture with AAV and Cas9 RNP electroporation were not yet determined except for mice and rats.

METHODS

All methods can be found in the accompanying Transparent Methods supplemental file.

SUPPLEMENTAL INFORMATION

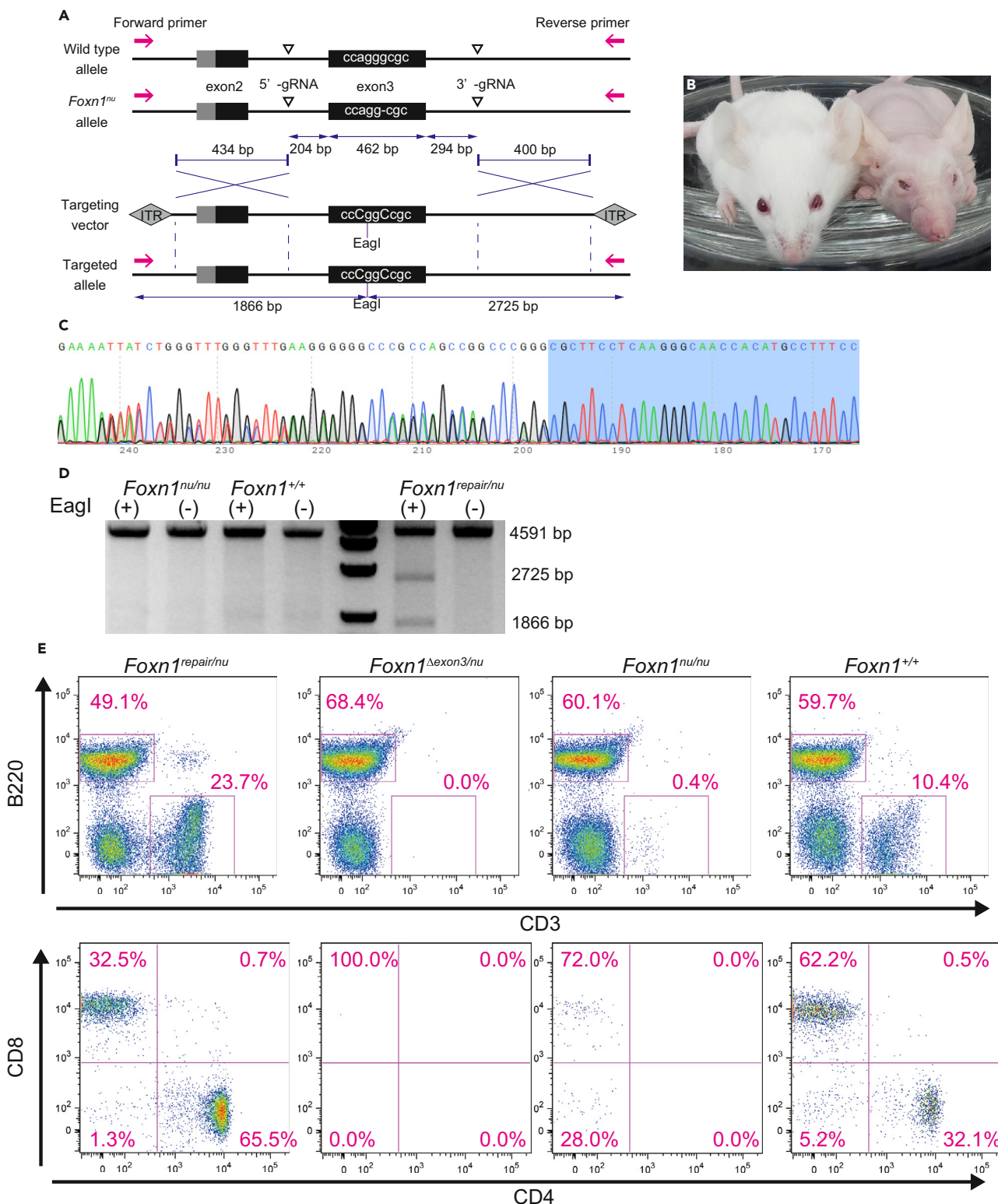Supplemental Information includes Transparent Methods, seven figures, and one table and can be found with this article online at https://doi.org/10.1016/j.isci.2018.10.030.

Figure 4. Correction of *Foxn1* Gene in Mouse Embryos by Exon Exchange

(A) Schematic representation of targeting strategy. A 1-bp deletion on exon 3 of *Foxn1[nu]* allele results in frameshift mutation. Two gRNAs were designed on introns 2 and 3 flanking exon 3 of *Foxn1* gene. Repair donor scAAV vector containing 960-bp gRNA-flanking region with corrected exon 3 sequence and 434-bp 5′ homology arm and 400-bp 3′ homology arm. Magenta arrows, mouse *Foxn1* primers (forward and reverse).

Figure 4. *Continued*

(B) Macroscopy of KSN/Slc-*Foxn1*$^{repaired/nu}$ (left) and KSN/Slc-*Foxn1*$^{nu/nu}$ (right).

(C) Representative of Sanger sequencing of exon 3 in KSN/Slc-*Foxn1*$^{repaired/nu}$. Two sequences were combined from *Foxn1*^{nu} mutation.

(D) Restriction fragment-length polymorphism analysis of *Foxn1*$^{repaired/nu}$. A 4,590- 4,591-bp amplicon of Foxn1-flanking homology arms and exon 3 were digested with EagI. Amplicon derived from *Foxn1*^{repaired} allele resulted in 1,866- and 2,725-bp products.

(E) Flow cytometry of peripheral blood white blood cells in KSN/Slc-*Foxn1*$^{repaired/nu}$, KSN/Slc-*Foxn1*$^{\Delta exon3/nu}$, KSN/Slc-*Foxn1*$^{nu/nu}$, and wild-type C57BL/6N mouse. Mature T cells were detected in KSN/Slc-*Foxn1*$^{repaired/nu}$, but neither in KSN/Slc-*Foxn1*$^{\Delta exon3/nu}$ nor in KSN/Slc-*Foxn1*$^{nu/nu}$. *Foxn1*$^{\Delta exon3}$, large deletion around exon 3, resulted from NHEJ between two gRNA targets.

See also Figure S7E and Table S1.

AUTHOR CONTRIBUTIONS

Conceptualization, N.M., E.M., T.Y., and H.N.; Methodology, N.M., E.M., H.S., F.S., and T.Y.; Investigation, N.M., E.M., H.S., M.K., A.O., and T.Y.; Resources, N.M., E.M., H.S., M.K., A.O., and T.Y.; Writing – Original Draft, N.M. and T.Y.; Writing – Review & Editing, N.M., E.M., F.S., T.Y. and H.N.; Supervision, T.Y. and H.N.; Funding Acquisition, T.Y. and H.N.

DECLARATION OF INTERESTS

The authors declare no competing interests.

REFERENCES

Abe, K.-i., Funaya, S., Tsukioka, D., Kawamura, M., Suzuki, Y., Suzuki, M.G., Schultz, R.M., and Aoki, F. (2018). Minor zygotic gene activation is essential for mouse preimplantation development. Proc. Natl. Acad. Sci. U S A 115, E6780–E6788.

Aida, T., Chiyo, K., Usami, T., Ishikubo, H., Imahashi, R., Wada, Y., Tanaka, K.F., Sakuma, T., Yamamoto, T., and Tanaka, K. (2015). Cloning-free CRISPR/Cas system facilitates functional cassette knock-in in mice. Genome Biol. 16, 87.

Bak, R.O., and Porteus, M.H. (2017). CRISPR-mediated integration of large gene cassettes using AAV donor vectors. Cell Rep. 20, 750–756.

Bane, D.P., James, J.E., Gradil, C.M., and Molitor, T.W. (1990). In vitro exposure of preimplantation porcine embryos to porcine parvovirus. Theriogenology 33, 553–561.

Chen, S., Lee, B., Lee, A.Y.-F., Modzelewski, A.J., and He, L. (2016). Highly efficient mouse genome editing by CRISPR ribonucleoprotein electroporation of zygotes. J. Biol. Chem. 291, 14457–14467.

Ellis, B.L., Hirsch, M.L., Barker, J.C., Connelly, J.P., Steininger, R.J., and Porteus, M.H. (2013). A survey of ex vivo/in vitro transduction efficiency of mammalian primary cells and cell lines with Nine natural adeno-associated virus (AAV1-9) and one engineered adeno-associated virus serotype. Virol. J. 10, 74.

Erles, K., Rohde, V., Thaele, M., Roth, S., Edler, L., and Schlehofer, J.R. (2001). DNA of adeno-associated virus (AAV) in testicular tissue and in abnormal semen samples. Hum. Reprod. 16, 2333–2337.

Gil-Farina, I., Fronza, R., Kaeppel, C., Lopez-Franco, E., Ferreira, V., D'Avola, D., Benito, A., Prieto, J., Petry, H., Gonzalez-Aseguinolaza, G., et al. (2016). Recombinant AAV integration is not associated with hepatic genotoxicity in nonhuman primates and patients. Mol. Ther. 24, 1100–1105.

Grieger, J.C., and Samulski, R.J. (2005). Packaging capacity of adeno-associated virus serotypes: impact of larger genomes on infectivity and postentry steps. J. Virol. 79, 9933–9944.

Hashimoto, M., Yamashita, Y., and Takemoto, T. (2016). Electroporation of Cas9 protein/sgRNA into early pronuclear zygotes generates non-mosaic mutants in the mouse. Dev. Biol. 418, 1–9.

Ikawa, M., Tanaka, N., Kao, W.W.Y., and Verma, I.M. (2003). Generation of transgenic mice using lentiviral vectors: a novel preclinical assessment of lentiviral vectors for gene therapy. Mol. Ther. 8, 666–673.

Izquierdo-Rico, M.J., Jiménez-Movilla, M., Llop, E., Pérez-Oliva, A.B., Ballesta, J., Gutiérrez-Gallego, R., Jiménez-Cervantes, C., and Avilés, M. (2009). Hamster zona pellucida is formed by four glycoproteins: ZP1, ZP2, ZP3, and ZP4. J. Proteome Res. 8, 926–941.

Jukam, D., Shariati, S.A.M., and Skotheim, J.M. (2017). Zygotic genome activation in vertebrates. Dev. Cell 42, 316–332.

Kaeppel, C., Beattie, S.G., Fronza, R., van Logtenstein, R., Salmon, F., Schmidt, S., Wolf, S., Nowrouzi, A., Glimm, H., von Kalle, C., et al. (2013). A largely random AAV integration profile after LPLD gene therapy. Nat. Med. 19, 889–891.

Kaneko, T., and Mashimo, T. (2015). Simple genome editing of rodent intact embryos by electroporation. PLoS One 10, e0142755.

McCarty, D.M., Monahan, P.E., and Samulski, R.J. (2001). Self-complementary recombinant adeno-associated virus (scAAV) vectors promote efficient transduction independently of DNA synthesis. Gene Ther. 8, 1248–1254.

Miura, H., Quadros, R.M., Gurumurthy, C.B., and Ohtsuka, M. (2017). Easi-CRISPR for creating knock-in and conditional knockout mouse models using long ssDNA donors. Nat. Protoc. 13, 195–215.

Miyasaka, Y., Uno, Y., Yoshimi, K., Kunihiro, Y., Yoshimura, T., Tanaka, T., Ishikubo, H., Hiraoka, Y., Takemoto, N., Tanaka, T., et al. (2018). CLICK: one-step generation of conditional knockout mice. BMC Genomics 19, 318.

Mroske, C., Rivera, H., Ul-Hasan, T., Chatterjee, S., and Wong, K.K. (2012). A capillary electrophoresis sequencing method for the identification of mutations in the inverted terminal repeats of adeno-associated virus. Hum. Gene Ther. Methods 23, 128–136.

Munk, M., Ladeira, L.O., Carvalho, B.C., Camargo, L.S.A., Raposo, N.R.B., Serapião, R.V., Quintão, C.C.R., Silva, S.R., Soares, J.S., Jorio, A., et al. (2016). Efficient delivery of DNA into bovine preimplantation embryos by multiwall carbon nanotubes. Sci. Rep. 6, 33588.

Nowrouzi, A., Penaud-Budloo, M., Kaeppel, C., Appelt, U., Le Guiner, C., Moullier, P., Kalle, C.v., Snyder, R.O., and Schmidt, M. (2012). Integration frequency and intermolecular recombination of rAAV vectors in non-human primate skeletal muscle and liver. Mol. Ther. 20, 1177–1186.

Sakuma, T., Nakade, S., Sakane, Y., Suzuki, K.-I.T., and Yamamoto, T. (2015). MMEJ-assisted gene knock-in using TALENs and CRISPR-Cas9 with the PITCh systems. Nat. Protoc. 11, 118–133.

Suzuki, K., Tsunekawa, Y., Hernandez-Benitez, R., Wu, J., Zhu, J., Kim, E.J., Hatanaka, F., Yamamoto, M., Araoka, T., Li, Z., et al. (2016). In vivo genome editing via CRISPR/Cas9 mediated homology-independent targeted integration. Nature 540, 144–149.

Vanroose, G., Nauwynck, H., Soom, A.V., Ysebaert, M.-T., Charlier, G., Oostveldt, P.V., and de Kruif, A. (2000). Structural aspects of the zona pellucida of in vitro-produced bovine embryos: a scanning electron and confocal laser scanning microscopic study. Biol. Reprod. 62, 463–469.

Wang, Z., Ma, H.I., Li, J., Sun, L., Zhang, J., and Xiao, X. (2003). Rapid and highly efficient transduction by double-stranded adeno-associated virus vectors in vitro and in vivo. Gene Ther. 10, 2105–2111.

Wiekowski, M., Miranda, M., and DePamphilis, M.L. (1991). Regulation of gene expression in preimplantation mouse embryos: effects of the zygotic clock and the first mitosis on promoter and enhancer activities. Dev. Biol. 147, 403–414.

Wu, Z., Yang, H., and Colosi, P. (2010). Effect of genome size on AAV vector packaging. Mol. Ther. 18, 80–86.

Yang, H., Wang, H., Shivalila, C.S., Cheng, A.W., Shi, L., and Jaenisch, R. (2013). One-step generation of mice carrying reporter and conditional alleles by CRISPR/Cas mediated genome engineering. Cell 154, 1370–1379.

Yoon, Y., Wang, D., Tai, P.W.L., Riley, J., Gao, G., and Rivera-Pérez, J.A. (2018). Streamlined ex vivo and in vivo genome editing in mouse embryos using recombinant adeno-associated viruses. Nat. Commun. 9, 412.

Yoshimi, K., Kunihiro, Y., Kaneko, T., Nagahora, H., Voigt, B., and Mashimo, T. (2016). ssODN-mediated knock-in with CRISPR-Cas for large genomic regions in zygotes. Nat. Commun. 7, 10431.

Supplemental Information

Intra-embryo Gene Cassette

Knockin by CRISPR/Cas9-Mediated Genome

Editing with Adeno-Associated Viral Vector

Naoaki Mizuno, Eiji Mizutani, Hideyuki Sato, Mariko Kasai, Aki Ogawa, Fabian Suchy, Tomoyuki Yamaguchi, and Hiromitsu Nakauchi
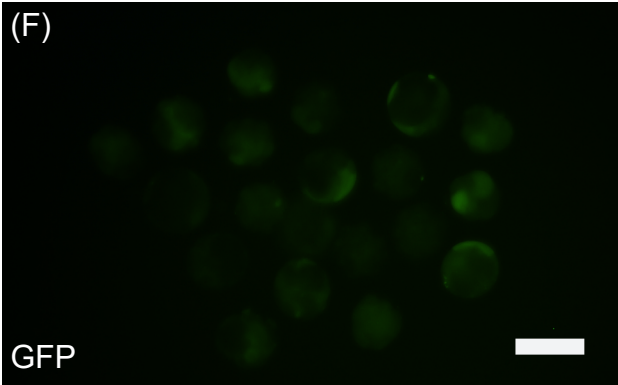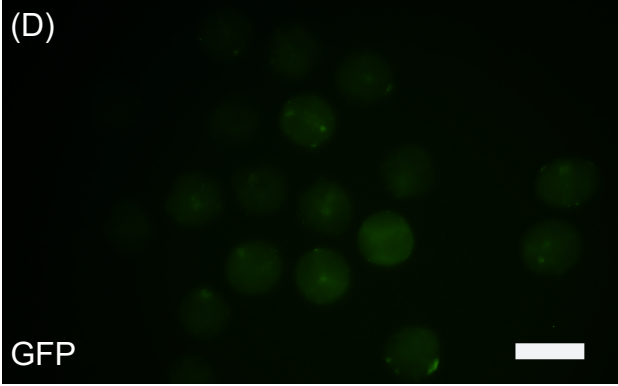
Figure S1

(A) BF

(B) GFP

(C) BF

(D) GFP

(E) BF

(F) GFP

(G) BF

(H) GFP

Figure S1. Related to Figure 1. Lentiviral vector-mediated transduction of mouse embryos.

Fertilized zygotes with zona pellucida co-cultured with CS-CAG-EGFP at the concentration of 1 ×

10^6 IU/mL showed no EGFP expression (A) (B). Microinjection of viral suspension at the

concentration of 1 × 10^8 IU/mL to perivitelline space resulted in EGFP expression, at morula (C)

(D) and blastocyst stages (E) (F). Lentiviral vector transduced embryos after zona pellucida

removal (G) (H). Scale bars, 100 μm.

Figure S2
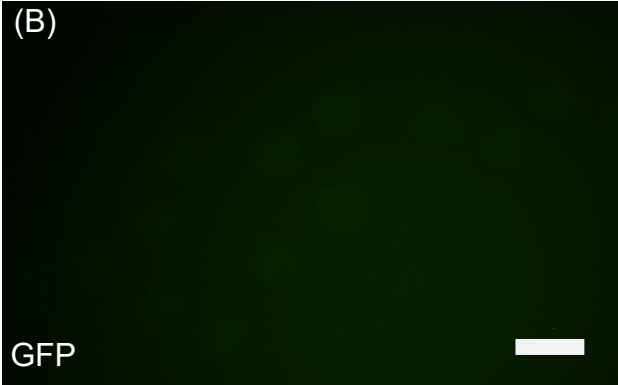

(A) BF

(B) GFP

(C) BF

(D) GFP

(E) BF

(F) GFP
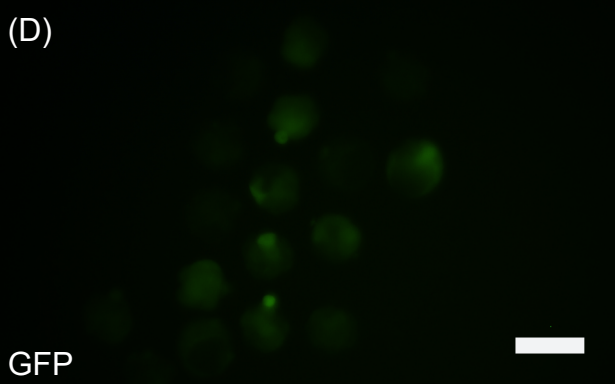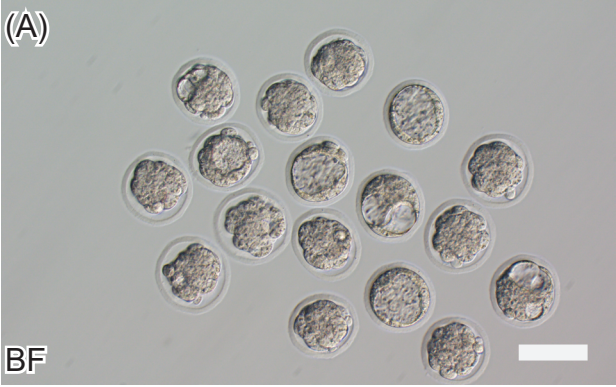
Figure S2. Related to Figure 1. Adenoviral vector-mediated transduction of mouse embryos.

Fertilized zygotes with zona pellucida co-cultured with AdEasy-CAG-EGFP at the concentration of

1×10^6 IU/mL showed no EGFP expression (A) (B). Microinjection of viral suspension at the

concentration of 3.6 $\times$ 10^8 IU/mL to perivitelline space resulted in EGFP expression at

morula/blastocyst stages (C) (D) compared with that of mock-transduced embryos (E) (F). Scale

bars, 100 μm.
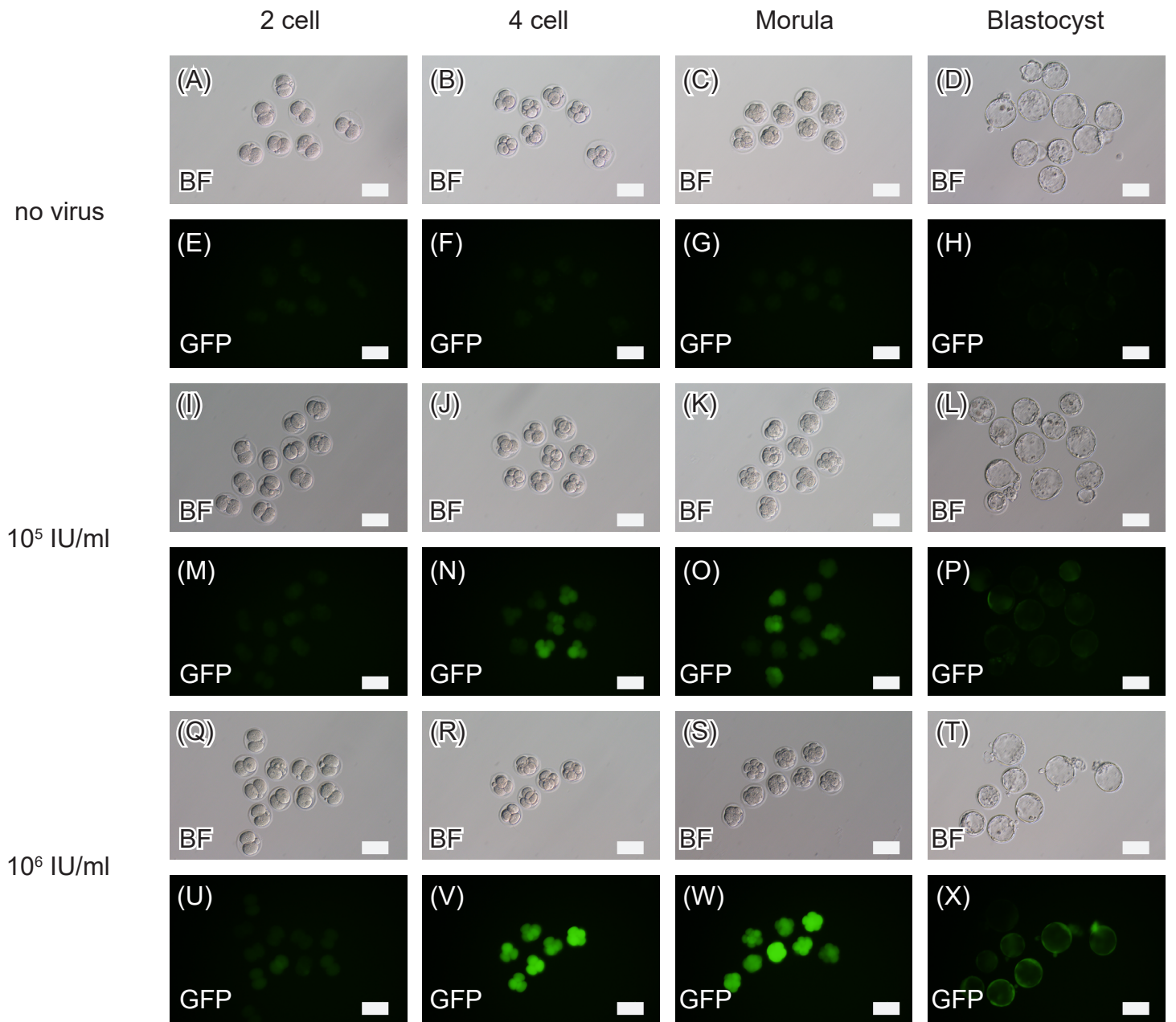
Figure S3

Figure S3. Related to Figure 1. Time course of the reporter gene transient expression following

AAV-mediated transduction in mouse embryogenesis. Zygotes of mice with zona pellucida were

co-cultured with EGFP expression scAAV6 (scAAV6-CAG-EGFP) at 1×10^5 IU/mL (I-P), at 1×10^6

IU/mL (Q-X), or without AAV (A-H) for 16 h. Embryos were cultured in vitro, and the expression of

EGFP was analyzed by fluorescence microscopy from 2-cell stage to blastocyst stage. Scale bars,

100 μm.

Figure S4

	Mouse	Rat	Bovine

no virus

(A) GFP

(B) GFP

(C) GFP

Serotype 1

(D) GFP

(E) GFP

(F) GFP

Serotype 2

(G) GFP

(H) GFP

(I) GFP

Serotype 6

(J) GFP

(K) GFP

(L) GFP
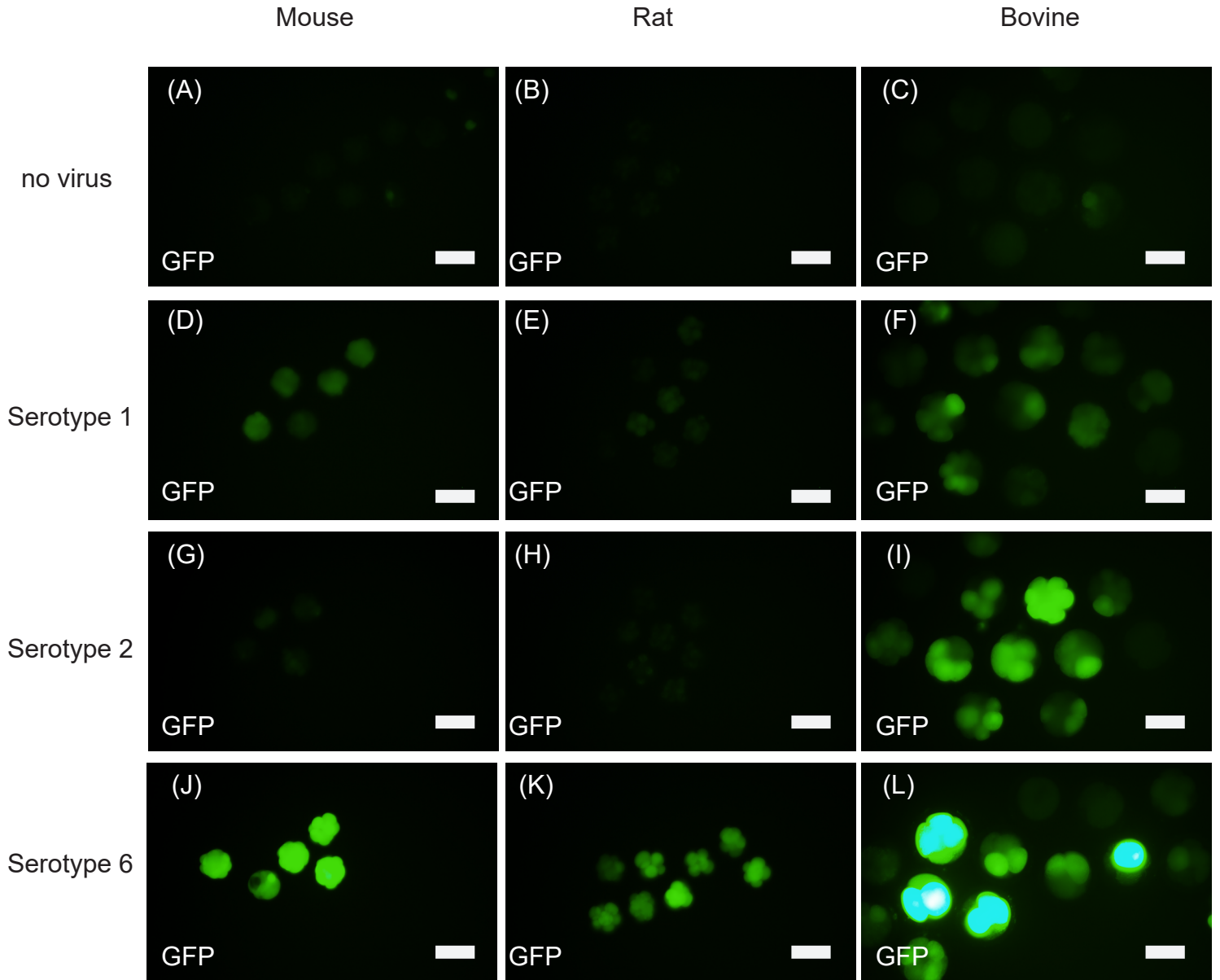
Figure S4. Related to Figure 1. Serotype specific AAV vector transduction of embryos in different species. Fertilized zygotes with zona pellucida co-cultured with scAAV-CAG-EGFP at a concentration of 3 × 10^8 vg/mL. (A-C) Negative control embryos. (D-F) Serotype 1 scAAV transduced embryos. (G-I) Serotype 2 scAAV transduced embryos. (J-L) Serotype 6 transduced embryos. EGFP expression were evaluated at morula/blastocyst stage of mouse embryos (A) (D) (G) (J), of rat embryos (B) (E) (H) (K) and of bovine embryos (C) (F) (I) (L). Scale bars, 100 μm.

Figure S5

(A)

5' arm

AGGGAGCTGCAGTGGAGTAGGCGGGGAGAAGGCCGCACCCTTCTCCGGAGGGGGGAGGGGAGTGTTGCAATACCTTTCTGGGAGTTCTCTGCTGCCTCCTGGCTTCTGAGGACCGCCCTAGGCCATTGACGTCA

3' arm

ACAACGCCCACACACCAGGTTAGCCTTTAAGCCTGCCCAGAAGACTCCCGCCCATCTTCTAGAAAGACTGGAGTTGCAGATCACGAGGGAAGAGGGGGAAGGGATTCTCCCAGGCCCACTAGTTTAAAAAACCTC

(B)

5' arm

GCGGCCGCGGCAGGCCCTCCGAGCGTGGTGGAGCCGTTCTGTGAGACAGCCGGGTACGAGTCGTGACGCTGGAAGGGGCAAGCGGGTGGTGGGCAGGAATGCGGTCCGCCCTGCAGCAACCGGAGGGGGAGGGAGAA

3' arm

ATTCCAAAAGGAACCACCTTTTACAGATGTGTACAATGACAAAATTTTAGTAAGCAGTAATCAATACCATGTGGCTCAATAATGAAATATACCTTTTAATGTCTTAAAATATCAGCCTGGCAATATGTAAGATACATCAG

Figure S5. Related to Figure 2. Precise insertion of knock-in cassettes in *Rosa26*-CAG-EGFP

knock-in mice. HDR was confirmed by Sanger sequencing of 5′ and 3′ junctional regions both

in scAAV-mediated knock-in mice (A) and ssAAV-mediated knock-in mice (B). Blue box, homology
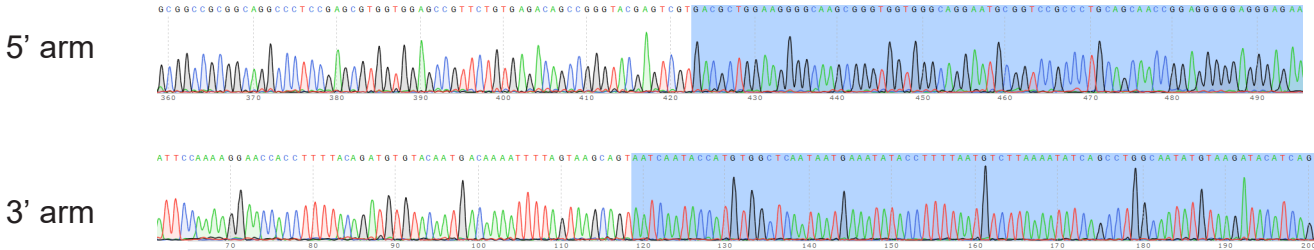
arm.

Figure S6

5' arm

3' arm
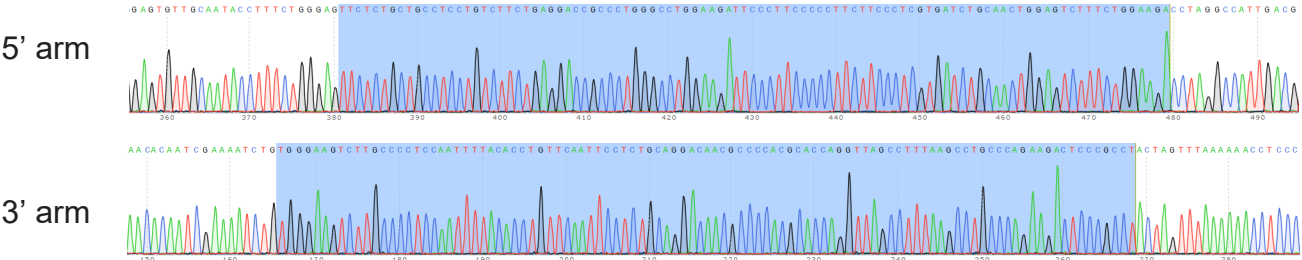
Figure S6. Related to Figure 3. Precise insertion of knock-in cassettes in *Rosa26*-CAG-EGFP

knock-in rats. HDR was confirmed by Sanger sequencing of 5′ and 3′ junctional regions. Blue

box, homology arm.

Figure S7

(A)

F1 offspring
with KI allele

F1 offspring
without KI allele

5' arm-CAG

EGFP-3' arm

(B)

F1 offspring
with KI allele

F1 offspring
without KI allele

5' arm-CAG

EGFP-3' arm

(C)

F1 offspring
without KI allele

F1 offspring
with KI allele

5' arm-CAG

EGFP-3' arm

(D)

(E)

F1 offspring
without *Foxn1*[repair] allele

F1 offspring
with *Foxn1*[repair] allele

EagI   (+)   (−)   (+)   (−)   (+)   (−)   (+)   (−)

4591 bp
2725 bp
1866 bp

Figure S7. Related to Figure 2, Figure 3 and Figure 4. Germline transmission of the knock-in
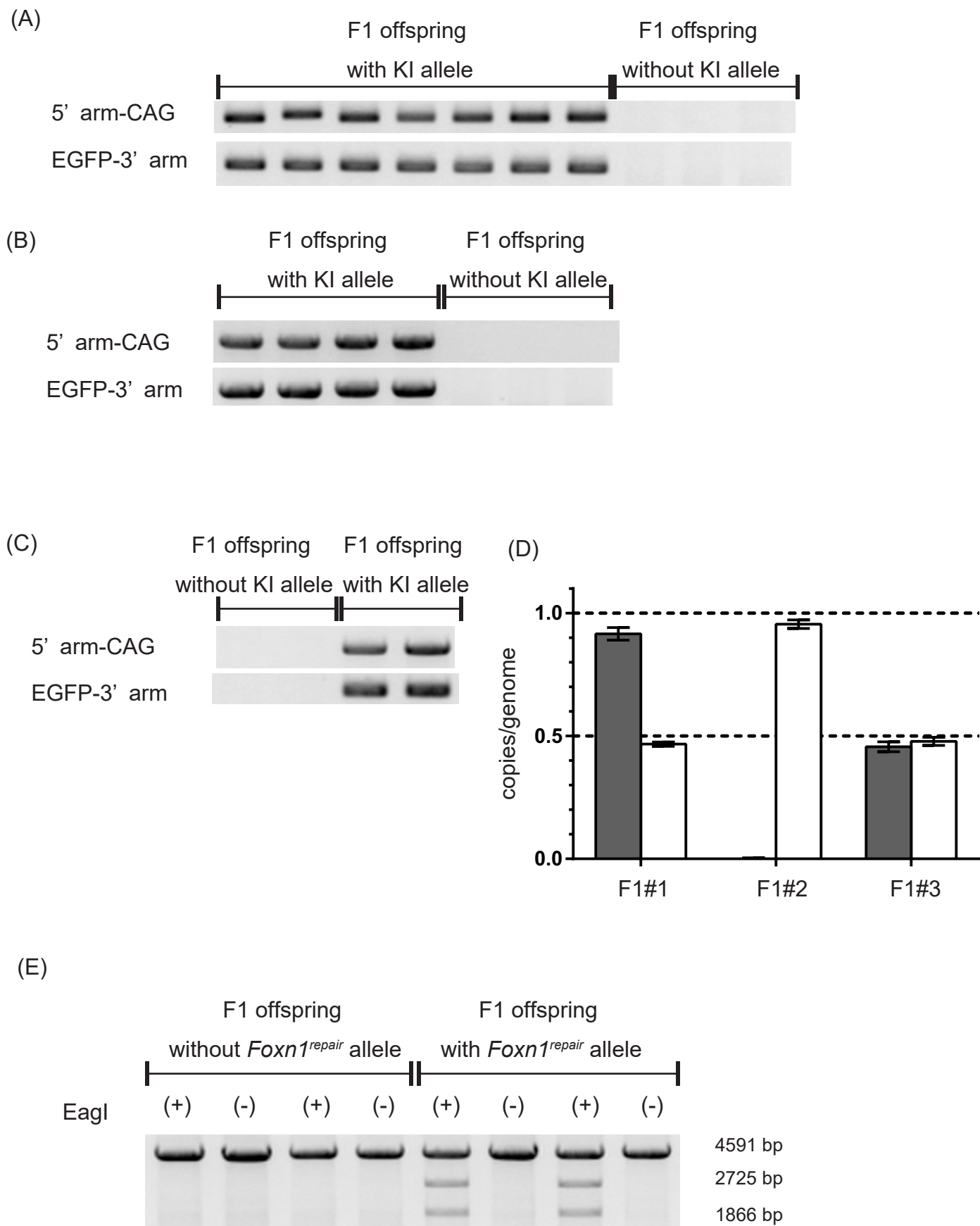
mice and rats. (A-B) Representative of genotyping PCR for N1 generation offspring in the mouse

Rosa26-CAG-EGFP knock-in strain. The founder mice with *Rosa26* CAG-EGFP allele introduced

by the donor scAAV6 (A) and the donor ssAAV6 (B) were bred to a wild-type C57BL/6N mouse.

Genotyping PCR was performed with primers flanking the 5′ and 3′ junctional regions. (C)

Representative of genotyping PCR for N1 generation offspring in the rat *Rosa26*-CAG-EGFP

knock-in strain. The founder rat with *Rosa26* CAG-EGFP allele introduced by the donor scAAV6

was bred to a wild-type Wistar rat. Genotyping PCR was performed with primers flanking the 5′

and 3′ junctional regions. (D) Droplet digital PCR analysis for N1 generation offspring in the rat

Rosa26-CAG-EGFP knock-in strain. Copy number of EGFP and rat *Rosa26* allele without

integration were quantified by droplet digital PCR. Absolute copies were normalized to copies of

reference genome targeting endogenous *Zeb2* locus and expressed as mean ± SEM (n = 4,

technical replicates). Gray column, EGFP copies/genome; open column, copies of un-inserted rat

Rosa26 allele/genome. (E) Representative of RFLP analysis for N1 generation offspring in the

Foxn1$^{repaired/nu}$ strain. The founder mouse with *Foxn1$^{repaired/nu}$* allele introduced by the donor

scAAV6 was bred to a *Foxn1$^{nu/nu}$* mouse. 4590-4591 bp amplicon of Foxn1 flanking homology

arms and exon 3 were digested with EagI. Amplicon derived from Foxn1repaired allele resulted in

1866 bp and 2725 bp products.

Table S1. Related to Figure 4. Knock-in efficiency of nude mouse offsprings after zygote genome editing with repair-donor AAV transduction

number of 2PN zygotes treated	number of zygotes on 2-cell stage	number of zygotes transferred	number of offsprings	number of knock-in offsprings	number of offsprings with large-deletion
92	79 (85.9)	79 (100)	16 (20.3)	3 (18.8)	9 (56.3)

Transparent Methods

Animals. C57BL/6N, B6D2F1, ICR and KSN/Slc mice were purchased from Japan SLC (Shizuoka, Japan). Wistar rats were purchased from Charles River Laboratories Japan (Yokohama, Japan). Bovine unfertilized eggs and bovine frozen semen were purchased from Research Institute for the Functional Peptides (Yamagata, Japan). All mice and rats were maintained in a 12 h light cycle. All animal experiments were approved by the Institutional Animal Care and Use Committee, and performed in accordance with the guidelines of the University of Tokyo and the National Institute for Physiological Sciences.

Targeting vector construction. Mouse *Rosa26* targeting scAAV vector plasmid, pscAAV-mRosa26-CAG-EGFP, was constructed by modification of pscAAV-CAG-GFP (a gift from Dr. Mark Kay, Addgene plasmid # 83279). *Rosa26* homology arms were amplified by PCR from genomic DNA, and inserted into the AvrII site and the SpeI site of pscAAV-CAG-GFP respectively by In-Fusion HD Cloning Kit (Clontech, Mountain View, CA, USA). Mouse *Rosa26* targeting ssAAV vector plasmid, pAAV-mRosa26-CAG-EGFP, was constructed by modification of pAAV-MCS2 (a gift from Dr. Steve Jackson, Addgene plasmid # 46954). The NotI site on pAAV-MCS2 was replaced with a SalI site by NEBuilder HiFi DNA Assembly Master Mix (New

England Biolabs, Massachusetts, MA, USA). Rosa26 homology arms were amplified by PCR from genomic DNA. 5' homology arm, 3' homology arm and CAG-EGFP cassette from pscAAV-CAG-EGFP were inserted into pUC19 by In-Fusion HD Cloning Kit. The plasmids were digested with SalI and MluI, and ligated by DNA Ligation Kit Mighty Mix (Takara Bio, Shiga, Japan). Rat *Rosa26* targeting scAAV vector plasmid, pscAAV-rRosa26-CAG-EGFP, was constructed by modification of pscAAV-CAG-GFP. Rat *Rosa26* homology arms were amplified by PCR from genomic DNA. 5' and 3' homology arms were inserted into the AvrII site and the SpeI site of pscAAV-CAG-GFP respectively by In-Fusion HD Cloning Kit. Rat *Rosa26* targeting ssAAV vector plasmid, pAAV-rRosa26-CAG-EGFP, was constructed by modification of pAAV-mRosa26-CAG-EGFP. Rat *Rosa26* homology arms were amplified by PCR from genomic DNA. 5' and 3' homology arms were inserted into the SalI-AvrII site and the SpeI-MluI site of pAAV-mRosa26-CAG-EGFP respectively by In-Fusion HD Cloning Kit. Mouse *Foxn1* targeting scAAV vector plasmid, pscAAV-Foxn1-nuEagI, was constructed by modification of pscAAV-CAG-GFP. 1 bp deletion of *Foxn1^{nu}* exon 3 was corrected by primer mutagenesis from KSN/Slc genomic DNA. Amplicons were inserted into pUC19 by In-Fusion HD Cloning Kit. Corrected sequences contain in-frame silent mutation to provide EagI site for RFLP analysis. Homology arms were amplified by PCR with modification to remove gRNA target sites, and

inserted to pUC19 by In-Fusion HD Cloning Kit. The plasmids were digested with AvrII and SpeI, and ligated by DNA Ligation Kit Mighty Mix.

Adeno-associated viral vector production. Recombinant AAV were produced by co-transfection of AAV vector plasmid and packaging plasmids. 293T cells were seeded at 4×10^6 per 10 cm dish one day before transfection, and cultured in DMEM (Sigma-Aldrich, St. Louis, MO, USA) supplemented with 10% fetal bovine serum (Gibco, Waltham, MA, USA) and 1% l-glutamine-penicillin-streptomycin (Sigma-Aldrich, St. Louis, MO, USA). Calcium phosphate was used to transfect the 293T cells with 10 µg AAV vector plasmid and 25 µg pDGM6 (a gift from Dr. David Russell). Culture medium was exchanged 16 h after transfection and incubated for 48 h. AAV were extracted by AAVpro Purification Kit (All Serotypes) (Takara Bio, Shiga, Japan) and concentrated in PBS by Amicon Ultra-4, 100 kDa (Merck Millipore, Darmstadt, Germany). scAAV titers were estimated by infectious efficiency of 293T cells and reported as IU/mL. ssAAV titer were determined from viral genome copy estimated by QX200 Droplet Digital PCR system (Bio-Rad Laboratories, Hercules, CA, USA) and reported as vg/mL (Lock et al., 2014).

Embryo manipulation. Mouse and rat embryos were prepared as described previously (Nagy,

2003). In brief, zygotes were obtained from superovulated B6D2F1 female mice mated with C57BL/6N male mice by oviduct perfusion. Surrounding cumulus cells were removed by short-term culture and pipetting in 0.1% hyaluronidase-containing M2 medium (Merck Millipore, Darmstadt, Germany). Zygotes were cultured in KSOM-AA medium (Merck Millipore, Darmstadt, Germany) for 1-4 h, and two-pronuclear zygotes were collected. Cas9 ribonucleoprotein were transfected by electroporation described below. After the electroporation, zygotes were transferred to KSOM-AA medium containing recombinant AAV vectors and incubated for 16-24 h. Embryos at the 2-cell stage were rinsed with M2 medium three times and transferred to oviducts of E0.5 pseudopregnant ICR females. For in vitro culture, embryos at 2-cell stage were transferred to fresh KSOM-AA medium, and incubated for 3-5 days. Parthenogenetic embryos were prepared by activation of unfertilized oocytes. Oocytes were collected from the oviduct of superovulated B6D2F1 females and incubated in Ca-free KSOM-AA medium with 10 mM SrCl2 (Wako, Osaka, Japan) and 5 mg/mL cytochalasin B (Sigma-Aldrich, St. Louis, MO, USA) for 6 h. Oocytes were washed three times with M2 medium and cultured in KSOM-AA medium. Parthenogenetic embryos were exposed to AAV for 1 h before activation, or 16-24 h after activation. For rat zygotes, superovulated Wistar female rats were mated overnight with Wistar male rats. Zygotes were retrieved from the oviduct, and the surrounding cumulus cells were

removed by short-term culture and pipetting in 0.1% hyaluronidase-containing M2 medium.

Zygotes were cultured in mR1ECM medium (Oh et al., 1998) supplemented with 4 mg/mL bovine

serum albumin (300–310 mOsm/L) for 1-4 h, and two-pronuclear zygotes were collected. Cas9

ribonucleoprotein were transfected by electroporation described below. After the electroporation,

zygotes were transferred to mR1ECM medium (Ark Resource, Kumamoto, Japan) containing

recombinant AAV vectors and incubated for 16-24 h. Embryos at the 2-cell stage were rinsed with

M2 medium three times and transferred to oviducts of E0.5 pseudopregnant Wistar females.

Bovine fertilized eggs were prepared by in vitro fertilization (Hosoe et al., 2017). Cumulus-oocyte

complexes collected from bovine ovary were in-vitro maturated for 24 h in IVMD101 medium

(Research Institute for the Functional Peptides, Yamagata, Japan), at 38.5°C in 5% CO_2.

Cumulus-oocyte complexes were transferred into IVF100 medium (Research Institute for the

Functional Peptides, Yamagata, Japan) and in vitro fertilized with bovine semen for 6 h at 38.5°C

in 5% CO_2. Cumulus cells surrounding the oocytes were removed by vortex mixing in 0.1%

hyaluronidase (Sigma-Aldrich, St. Louis, MO, USA), and oocytes with a second polar body were

incubated in IVD101 medium (Research Institute for the Functional Peptides, Yamagata, Japan)

for 12 h, at 38.5°C in 5% CO_2 and 5% O_2. Zygotes were transferred to IVD101 medium containing

recombinant AAV vectors and incubated for 16-24 h. Zygotes were washed with IVD101 medium

three times, and cultured in IVD101 medium for 7 days, at 38.5°C in 5% CO_2 and 5% O_2.

Cas9 ribonucleoprotein electroporation. Cas9 ribonucleoproteins were introduced to zygotes

of mice and rats as described previously (Hashimoto et al., 2016). In brief, two-pronuclear zygotes

were washed three times with Opti-MEM I medium (Gibco, Waltham, MA, USA). 20-30 zygotes

were transferred into 5 µl Opti-MEM I medium containing 100 ng/µl Cas9 protein (IDT, Skokie, IL,

USA) and 200 ng/µl annealed gRNA complex on LF501PT1-10 electrode (BEX, Tokyo, Japan).

The gRNA complex was prepared by annealing of 100 µM crRNA (IDT, Skokie, IL, USA) and 100

µM tracrRNA (IDT, Skokie, IL, USA). The gRNA targets were as follows: mouse *Rosa26*,

5'-GGATTCTCCCAGGCCCAGGG-3'; rat *Rosa26*, 5'-GAGTCTTTCTGGAAGATAGG-3'; mouse

Foxn1 5'-gRNA, 5'-GCTGATGGGTTCCATATCTG-3'; mouse *Foxn1* 3'-gRNA,

5'-CAGGTGAGGGAAGCTCATGA-3'. Electroporation was performed with Genome Editor (BEX,

Tokyo, Japan) on the following conditions. B6D2F1×B6 mouse zygotes, 25 V, 3 ms ON, 97 ms

OFF, Pd Alt 4 times; KSN mouse zygotes, 25 V, 3 ms ON, 97 ms OFF, Pd Alt 3 times; Wistar rat

zygotes, 30 V, 3 ms ON, 97 ms OFF, Pd Alt 4 times.

Genotyping. Genotyping PCR of offspring was performed with crude lysate of the animals' ear,

and extracted genomic DNA purified by QIAamp DNA Blood Mini Kit (Qiagen, Hilden, Germany).

Genotyping of blastocysts was performed with crude lysate. For crude lysate, samples were

incubated in 20 mM Tris-HCl (pH8.0), 100 mM NaCl, 5 mM EDTA, 0.1% SDS, 200 µg/mL

Proteinase K, at 60°C for 5 min to 24 h, followed by 98°C Proteinase K heat-inactivation for 2 min.

Genomic PCR was performed with Tks Gflex DNA Polymerase (Takara Bio, Shiga, Japan) and

the following primers: 5' junction of mouse *Rosa26-CAG-EGFP* knock-in, forward

5'-GTTCGTGCAAGTTGAGTCCAT-3', reverse 5'-GCCAAGTAGGAAAGTCCCATAA-3'; 3'

junction of mouse *Rosa26-CAG-EGFP* knock-in, forward 5'-CACTACCTGAGCACCCAGTC-3',

reverse 5'-GTCTAACTCGCGACACTGTA-3'; 5' junction of rat *Rosa26-CAG-EGFP* knock-in,

forward 5'-ACTACTGTGTTGGCGGACTG-3', reverse 5'-GCCAAGTAGGAAAGTCCCATAA-3'; 3'

junction of mouse *Rosa26-CAG-EGFP knock-in*, forward 5'-CACTACCTGAGCACCCAGTC-3',

reverse 5'-ACTGTAGCAAGGATCGCAAGTG-3'; mouse *Foxn1*, forward 5'-

GCTGCTGTCAGGGATGAACT-3', reverse 5'- TGAGACTCCCTAGCCTCCAC -3'.

Flow cytometry. Peripheral blood was collected from the retro-orbital venous plexus into

heparinized capillary tubes. After erythrocyte lysis with ACK lysis buffer (150 mM ammonium

chloride, 10 mM potassium bicarbonate, 10 µM EDTA disodium), cells were stained with

antibodies at 4°C for 30 min. Flow cytometry was performed on FACSCanto II (BD Biosciences, San Jose, CA, USA). Collected data were analyzed with FlowJo software (BD Biosciences, San Jose, CA, USA).

Copy number estimation by digital PCR. Copy numbers of *EGFP* and un-inserted *Rosa26* alleles in the *Rosa26* CAG-EGFP knock-in rats were estimated by the QX200 Droplet Digital PCR system (Bio-Rad Laboratories, Hercules, CA, USA). The copy numbers were normalized to genome copies estimated from *Zeb2* locus. Genomic DNA was extracted from peripheral blood by QIAamp DNA Blood Mini Kit (Qiagen, Hilden, Germany). 30-100 µg genomic DNA per 20 µl reaction mixture was digested with BamHI and MfeI. BamHI site is located between CAG-promoter and EGFP. MfeI site is located on SV40pA downstream of EGFP. This digestion discriminate each EGFP even in case of concatemeric integration.Primers and the probe for EGFP are designed on EGFP. In order to determine how many Rosa26 alleles are mutant with insertions, we measured un-inserted *Rosa26* allele. *Rosa26* primers and the probe are designed on the following positions from gRNA break point: forward primer -203 nt to -180 nt, reverse primer +58 nt to + 79 nt, probe -113 nt to -90 nt. Wild-type *Rosa26* allele and mutant allele with short deletion < -57 bp contribute to templates for ddPCR. There are complementary sequences

with *Rosa26* primers and the probe on the knock-in allele. But the digestion dissects it between the probe site and the reverse primer site. Primers and probes (IDT, Skokie, IL, USA) were as follows: *EGFP* ddPCR primer F 5'-CTGCCCGACAACCACTAC-3', *EGFP* ddPCR primer R 5'-TCGTCCATGCCGAGAGT-3', *EGFP* ddPCR probe 5'-6-FAM/AGGACCATG/ZEN/TGATCGCGCTTCTC/IABkFQ-3'; *rRosa26* ddPCR primer F 5'-TCGGTTTGAGTTATCATTAAGGGA-3', *rRosa26* ddPCR primer R 5'-TACACCTGTTCAATTCCTCTGC-3', *rRosa26* ddPCR probe 5'-6-FAM/ACCTTTCTG/ZEN/GGAGTTCTCTGCTGC/IABkFQ-3'; *Zeb2* ddPCR primer F 5'-GGATGGGGAATGCAGCTCTT-3', *Zeb2* ddPCR primer R 5'-AGTGCGGCAGAATACAGCA-3', *Zeb2* ddPCR probe 5'-HEX/TGATGGGTT/ZEN/GTGAAGGCAGCTGCACCT/IABkFQ-3'.

Supplemental References

Hashimoto, M., Yamashita, Y., and Takemoto, T. (2016). Electroporation of Cas9 protein/sgRNA into early pronuclear zygotes generates non-mosaic mutants in the mouse. Developmental Biology *418*, 1-9.

Hosoe, M., Inaba, Y., Hashiyada, Y., Imai, K., Kajitani, K., Hasegawa, Y., Irie, M., Teramoto, H., Takahashi, T., and Niimura, S. (2017). Effect of supplemented sericin on the development, cell number, cryosurvival and number of lipid droplets in cultured bovine embryos. Animal Science Journal *88*, 241-247.

Lock, M., Alvira, M.R., Chen, S.-J., and Wilson, J.M. (2014). Absolute Determination of Single-Stranded and Self-Complementary Adeno-Associated Viral Vector Genome Titers by Droplet Digital PCR. Human Gene Therapy Methods *25*, 115-125.

Nagy, A. (2003). Manipulating the mouse embryo a laboratory manual (New York: Cold Spring Harbor Laboratory Press).

Oh, S.-H., Miyoshi, K., and Funahashi, H. (1998). Rat Oocytes Fertilized in Modified Rat 1-Cell Embryo Culture Medium Containing a High Sodium Chloride Concentration and Bovine Serum Albumin Maintain Developmental Ability to the Blastocyst Stage. Biology of Reproduction *59*, 884-889.